physchem

MDPI

Article

Modeling the Performance of Glass-Cover-Free Parabolic Trough Collector Prototypes for Solar Water Disinfection in Rural Off-Grid Communities

Fernando Aricapa [1,2], Jorge L. Gallego [3,*], Alejandro Silva-Cortés [4], Claudia Díaz-Mendoza [1] and Jorgelina Pasqualino [1]

1 GISAH Research Group, Environmental Engineering Program, Universidad Tecnológica de Bolívar Campus Tecnológico, km 1 vía Turbaco Cartagena, Cartagena de Indias 130011, Colombia; faricapa@tecnologicocomfenalco.edu.co (F.A.); cdiaz@utb.edu.co (C.D.-M.); jpasqualino@utb.edu.co (J.P.)
2 GIA Research Group, Department of Engineering, Fundación Universitaria Tecnológico Comfenalco, Cartagena de Indias 130015, Colombia
3 Biodiversity Biotechnology and Bioengineering Research Group GRINBIO, Department of Engineering, University of Medellin, Medellín 050026, Colombia
4 Department of Management Sciences, Instituto Tecnológico Metropolitano, Medellín 050013, Colombia; alejandrosilva@itm.edu.co
* Correspondence: jlgallego@udemedellin.edu.co

Abstract

In regions with abundant solar energy, solar water disinfection (SODIS) offers a sustainable strategy to improve drinking water access, especially in rural, off-grid communities. This study presents a numerical modeling approach to assess the thermal and microbial disinfection performance of glass-free parabolic trough collectors (PTCs). The model integrates geometric sizing, one-dimensional thermal energy balance, and first-order microbial inactivation kinetics, supported by optical simulations in SolTRACE 3.0. Simulations applied to a representative case in the Colombian Caribbean (Gambote, Bolívar) highlight the influence of rim angle, focal length, and optical properties on system efficiency. Results show that compact PTCs can achieve fluid temperatures above 70 °C and effective pathogen inactivation within short exposure times. Sensitivity analysis identifies key geometric and environmental factors that optimize performance under variable conditions. The model provides a practical tool for guiding the design and local adaptation of SODIS systems, supporting decentralized, low-cost water treatment solutions aligned with sustainable development goals. Furthermore, it offers a framework for future assessments of PTC implementations in different climatic scenarios.

Keywords: SODIS; parabolic trough collector; thermal efficiency; drinking water; solar thermal energy

Check for updates

Academic Editor: Carlos A. Nieto De Castro

Received: 19 December 2025
Revised: 9 January 2026
Accepted: 28 January 2026
Published: 2 February 2026

Copyright: © 2026 by the authors. Licensee MDPI, Basel, Switzerland. This article is an open access article distributed under the terms and conditions of the Creative Commons Attribution (CC BY) license.

1. Introduction

Solar energy is a renewable, accessible, and abundant resource available in most climatic zones. Its potential to generate thermal and electrical energy extends to crucial applications such as the inactivation of waterborne pathogens through direct ultraviolet (UV) and indirect infrared (IR) radiation mechanisms [1]. Among the most impactful uses of solar energy is its role in water disinfection, known as solar water disinfection (SODIS), which offers a practical, low-cost, and effective method to combat microbial contamination, particularly in underserved rural regions [2].

Globally, contaminated drinking water remains a major health challenge, contributing to approximately 1.5 million deaths annually, primarily due to diarrheal diseases caused by pathogens like *Escherichia coli*, *Enterococcus faecalis*, and various protozoa and viruses, which remain especially high in low- and lower-middle-income countries [3]. Conventional water disinfection approaches such as chlorination are effective but may lead to the formation of harmful disinfection byproducts such as trihalomethanes, which pose carcinogenic risks with prolonged exposure [4]. In contrast, SODIS utilizes solar radiation and ambient heat to inactivate pathogens in low-turbidity water, aligning with Sustainable Development Goals (SDGs) 6 and 7: clean water and affordable clean energy [5].

Recent research has focused on increasing the efficiency of solar disinfection systems through reactor design improvements and advanced materials. Innovations such as compound parabolic collectors (CPCs) and parabolic trough collectors (PTCs) are now employed to intensify solar concentration and raise water temperatures, enhancing the synergistic effects of thermal and photonic disinfection [6]. These technologies reduce disinfection time while improving microbial kill rates. Additionally, the integration of photocatalysts, particularly titanium dioxide (TiO_2), has proven effective in accelerating microbial inactivation through the production of reactive oxygen species under UV exposure [7]. The next generation of solar water disinfection systems increasingly incorporates nanomaterials to combine photothermal and photocatalytic effects [8].

Parabolic trough collectors (PTCs) in particular stand out for their ability to achieve medium to high temperatures as these systems use reflective surfaces to focus sunlight onto a linear receiver tube, significantly increasing thermal energy density [6]. The resulting temperature rise accelerates the inactivation of resilient pathogens through a dual mechanism of UV-induced photolysis and thermally induced denaturation, with studies confirming that temperatures above 60 °C can effectively eliminate most waterborne pathogens, including *Salmonella*, *Giardia*, and *Cryptosporidium* [9].

The design and efficiency of PTCs are influenced by several geometric parameters: rim angle, focal distance, aperture width, and receiver diameter, which control the intensity and distribution of solar radiation on the receiver, ultimately determining the collector's thermal efficiency [10]. Operational factors like flow rate, solar angle, and ambient temperature also affect heat transfer performance [11,12]. Modern computational modeling enables simulation of these parameters via energy balance and heat transfer equations, offering a robust framework for system optimization [9,13].

SODIS is inherently a synergistic process, leveraging both the germicidal effects of UV-A and UV-B radiation and the denaturation effects of sub-boiling thermal energy [7]. However, environmental factors such as irradiance, turbidity, wind speed, and initial water temperature significantly influence the efficacy of disinfection [14]. Thus, one of the key challenges in SODIS research is maximizing efficiency under variable atmospheric conditions, such as cloud cover or seasonal sun angles. To overcome these issues, new studies explore the use of photosensitizing materials, such as ruthenium complexes immobilized in solar reactors, which generate singlet oxygen upon solar exposure, an advanced oxidative mechanism proven effective in pathogen inactivation [15].

Despite this progress, most commercial PTC-based SODIS systems include a glass envelope around the receiver tube, primarily to reduce convective heat losses and enhance thermal isolation [16]. By enclosing the absorber in a glass tube, the system minimizes the influence of wind and ambient air, thereby lowering the overall heat loss coefficient, while in high-performance designs, this glass enclosure may be coupled with a vacuum-sealed gap between the receiver and the glass to further suppress both convective and conductive losses [6,17]. This configuration significantly improves thermal efficiency, particularly in high-temperature applications, by preserving more of the concentrated solar energy within

the heat transfer fluid (HTF), and anti-reflective coatings are often applied to the glass surface to maximize solar transmittance [18,19]. However, optical loss could be an issue with the inclusion of a glass cover as all solar radiation reflected from the concentrator must pass through the glass before reaching the receiver. Even under optimal conditions, this introduces a transmittance loss of about 10% due to reflection and absorption, and the loss can be greater if the glass surface becomes dusty or degraded [20]. These optical losses directly reduce the net energy delivered to the HTF, potentially limiting the disinfection efficiency during marginal sunlight conditions. Furthermore, the glass cover adds material cost, weight, and complexity to the system's assembly and maintenance, which may hinder widespread deployment in low-resource settings [11,21].

In terms of heat transfer dynamics, energy absorbed by the receiver is partly lost by conduction to supporting structures, re-radiated back toward the glass envelope, or dissipated via convection to the surrounding air [20]. When glazing is used, some of this re-radiated and convective heat can be reabsorbed or retained within the system, but energy still escapes through the glass by convection to the ambient and radiation to the sky. Studies comparing glazed and unglazed receivers have found that while glazing improves heat retention at lower mass flow rates, its performance advantage diminishes at higher flow rates (e.g., above 0.024 kg/s), where increased thermal transport reduces residence time and minimizes external losses [12].

In this context, the trade-off between thermal insulation and optical efficiency must be carefully balanced. In specific cases, such as low-cost SODIS systems in sunny, low-wind regions, unglazed designs may offer a more viable solution, provided that the thermal and microbial targets can be met with simplified configurations. Thus, developing glass-free PTC designs that maintain thermal efficiency is a critical step toward scalable, low-cost disinfection solutions [22]. Therefore, recent research highlights the critical role of modeling tools in assessing and optimizing glass-free parabolic trough collector (PTC) systems for solar water disinfection [23]. These tools enable predictive simulations of absorber geometry, flow conditions, and heat distribution, facilitating accurate performance evaluation under varying local environmental conditions [24,25].

By incorporating site-specific parameters, modeling approaches help adapt system designs to regional climates, ensuring both thermal efficiency and microbial inactivation [24,26]. As a result, they provide a robust, cost-effective, and data-driven framework for developing high-efficiency, glass-free SODIS systems. This research aims to evaluate, through numerical modeling, the thermal and disinfection performance of small-scale, glass-free parabolic trough collector (PTC) prototypes for solar water disinfection (SODIS) applications under the environmental conditions of Gambote, Bolívar, a representative rural community in the Colombian Caribbean. By combining optical simulation, heat transfer modeling, and microbial inactivation kinetics, the study identifies key design and environmental parameters that influence the efficiency of compact, low-cost PTC systems adapted for decentralized water treatment in resource-limited settings with high solar potential, offering a viable solution to improve global access to clean water.

2. Materials and Methods

2.1. Model Overview

This study presents a numerical modeling approach to evaluate the thermal and disinfection performance of different glass-free parabolic trough collector (PTC) prototypes for solar water disinfection (SODIS) applications. The modeling process integrates three key components: (i) geometric and optical simulation of solar concentration using SolTrace 3.0 to analyze ray paths and optical efficiency under varying rim angles and focal lengths; (ii) a one-dimensional thermal model developed in MATLAB, based on energy balance

equations, to estimate water temperature along the receiver; (iii) a microbial inactivation sub-model applying first-order kinetics to simulate the decrease in selected pathogens based on time–temperature exposure. The model was applied to a case study in Gambote, Bolívar (Colombia), using representative meteorological data to assess performance under real environmental conditions, and a sensitivity analysis was conducted to evaluate the suitability of different prototype configurations. The components of the model and theoretical framework are described in detail in the following subsections.

2.2. PTC Prototypes and Modelling of Geometric Parameters

Parabolic trough collectors (PTCs) are a type of line-focus solar thermal technology that use a reflective parabolically shaped surface to concentrate direct solar radiation onto a receiver tube located along the focal line [16]. This configuration enables efficient transformation of solar energy into thermal energy, making PTCs suitable for a variety of low to medium-temperature applications including water disinfection, industrial heat processes, and residential heating systems. The absence of a glass envelope in certain PTC designs simplifies construction and reduces costs, while still maintaining thermal performance when appropriately sized.

A glass-free PTC is composed of three main elements: (i) the parabolic reflector, typically made of polished aluminum or other reflective materials; (ii) the absorber tube or receiver, usually constructed from copper, aluminum, or stainless steel with a selective coating to enhance absorptivity; (iii) the mechanical support and tracking system, which ensures the aperture continuously follows the solar path [6,27]. The heat transfer fluid (HTF) flows through the absorber tube, collecting thermal energy concentrated by the reflector. While larger receiver diameters can increase energy absorption, they may also introduce greater convective losses if not properly optimized, especially in systems without a protective glass envelope.

To evaluate performance under varying geometric designs, a set of small-scale PTC prototypes from the literature was selected. These prototypes were analyzed using general equations for geometric configuration (see material: Geometric Factors and Design Equations of the Parabolic Trough Collector). Software MATLAB 9.3. (MathWorks, Inc., Natick, MA, USA) was used to simulate the optical and thermal behavior of each prototype under different design scenarios, supporting performance prediction and the identification of optimal geometries for solar water disinfection applications.

2.3. Thermal Model Development

2.3.1. Conceptual Model

To evaluate the thermal performance of a glass-free parabolic trough collector (PTC), it is essential to quantify the heat transfer processes driven by direct solar radiation. In this model, three primary heat transfer mechanisms are considered: conduction, convection, and radiation, under the assumption of uniform irradiance over the outer surface of the absorber tube and a consistent distribution of temperature and heat flux along the receiver [27] (Figure 1). These processes are governed by the thermal properties of the heat transfer fluid (HTF), the collector's geometry, and the thermal and optical characteristics of the materials in contact. A one-dimensional energy balance model was applied, which is suitable for low- to medium-temperature collectors and receiver tubes shorter than 100 m [27–29]. This approach allows a simplified yet sufficiently accurate prediction of the longitudinal thermal profile along the receiver. Although it does not account for certain real-world effects such as optical errors, tracking deviations, dust accumulation, and partial shading, the model offers a reliable approximation of the collector's thermal performance under ideal conditions.

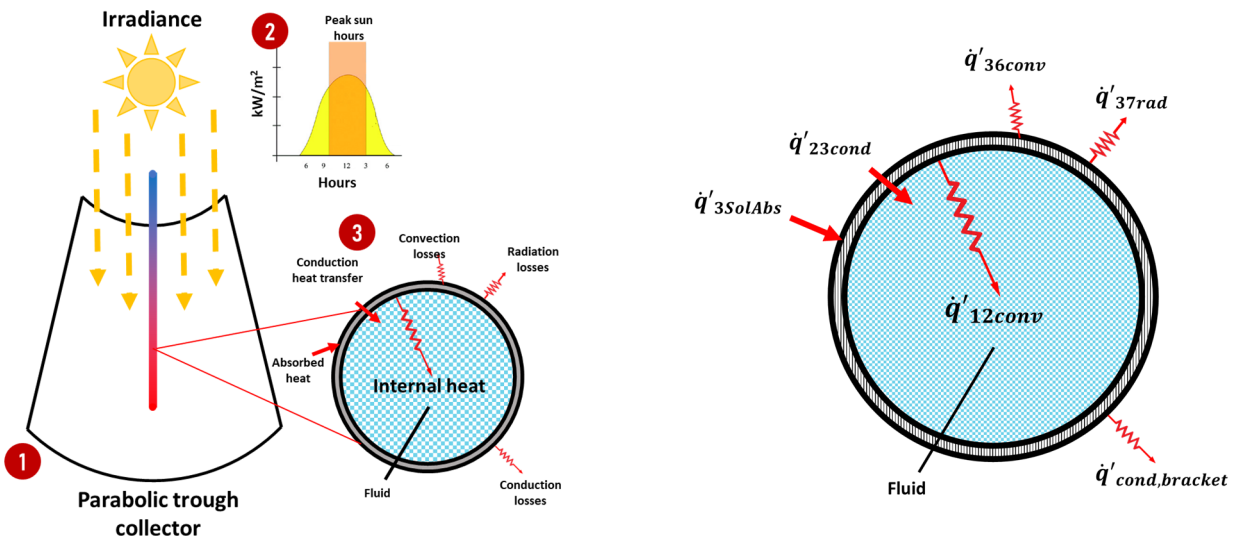

Figure 1. Heat transfer mechanisms in a glass-free parabolic trough solar collector. (1) Solar rays incident on the collector surface, (2) Distribution of solar irradiance and peak sun hours throughout the day, (3) Cross-sectional view of the receiver and one-dimensional heat transfer balance.

The governing equations applied include Fourier's law for conduction, Newton's law of cooling for convection, and the Stefan–Boltzmann law for radiation, each adapted to the thermal behavior of cylindrical solar collectors. The relevant heat transfer modes and paths are summarized in Table 1, following the energy balance formulation [27].

Table 1. Heat Transfer Paths in the Receiver Tube Based on One-Dimensional Energy Balance.

Thermal Flow (Wm^{-1})	Heat Transfer Mode	Transfer Trajectory	
		From	To
q12conv	Convection	Inner surface of the absorber tube	Heat transfer fluid (HTF)
q23cond	Conduction	Outer surface of absorber tube	Inner surface of absorber tube
q3SolAbs	Solar irradiance absorption	Incident solar radiation	Outer surface of absorber tube
q36conv	Convection	Outer surface of absorber tube	Ambient air
q37rad	Radiation	Outer surface of absorber tube	Sky
qcond, bracket	Conduction	Outer surface of absorber tube	Support brackets
qHeatLoss	Convection and radiation	Receiver system	Ambient air and sky

Adapted from Forristall (2003) [27].

The model begins by calculating the internal convective heat transfer between the absorber tube and the heat transfer fluid (HTF). This is determined using Newton's law of cooling, expressed in Equation (1):

$$\dot{q}'_{12conv} = h_1 D_i \pi \left(T_{cub} - T_{htf} \right) \tag{1}$$

where h_1 is the convective heat transfer coefficient, D_i is the inner diameter of the receiver, and T_{cub} and T_{htf} are the temperatures of the tube wall and fluid, respectively. The convective heat transfer coefficient h_1 is derived from the Nusselt number, as shown in Equation (2):

$$h_1 = Nu_D \frac{k_1}{D_i} \tag{2}$$

where k_1 is the thermal conductivity of the fluid at the mean temperature.

To determine Nu_D, the model first evaluates the flow regime using the Reynolds number. For turbulent flow conditions ($R_e > 2300$), the Gnielinski correlation is used, as

given by Equation (3). For laminar flow (R_e < 2300), the model simplifies the calculation by assigning a constant Nusselt number Nu_D = 4.36.

$$Nu_D = \frac{\frac{f_2}{8(Re_1-1000)Pr_1}}{1+12.7\sqrt{\frac{f_2}{8}}\left(Pr_1^{\frac{2}{3}}-1\right)}\left(\frac{Pr_1}{Pr_2}\right)^{0.11} \tag{3}$$

The friction factor f_2 is calculated in Equation (4):

$$f_2 = \left(1.82\log_{10}(Re_1) - 1.64\right)^{-2} \tag{4}$$

External convective heat loss to the ambient environment is also considered, as this represents a significant loss mechanism, especially under wind-exposed conditions [30]. The heat transfer from the outer surface of the absorber to ambient air is calculated using Newton's cooling law, shown in Equation (5):

$$\dot{q}\prime_{36conv} = h_2 D_e \pi (T_{cub} - T_{amb}) \tag{5}$$

Here, h_2 represents the heat transfer coefficient of air, which is calculated based on the Nusselt number for external flow using Equation (6):

$$h_2 = \frac{k_{air}}{D_e} Nu_a \tag{6}$$

This correlation is valid for a wide range of conditions, specifically when the Prandtl number falls within 0.7 < Pr < 500 and the Reynolds number is 1 < R_e < 106. To determine Nu_a, the model applies the Zhukauskas correlation, which is suitable for forced convection over a horizontal isothermal cylinder [31] and is expressed in Equation (7):

$$Nu_a = CRe_2^m Pr_{air}^n \left(\frac{Pr_{air}}{Pr_{air2}}\right)^{1/4} \tag{7}$$

The thermophysical properties of air are evaluated at ambient temperature to ensure accurate estimation of convective heat losses under typical environmental conditions. The Nusselt number for external forced convection is determined using the Zhukauskas correlation, which depends on R_e and the Prandtl number (Pr). The corresponding empirical coefficients—C and m—are selected based on the Reynolds number range (Table S1). Specifically, the exponent n takes a value of 0.37 for $Pr \leq 10$, and 0.36 for $Pr > 10$, reflecting typical conditions for air in solar thermal applications.

2.3.2. Radiative Heat Transfer Between the Receiver Surface and the Sky

Radiative heat loss from the outer surface of the absorber to the sky is primarily driven by the temperature difference between these two bodies. The effective sky temperature is typically approximated as 8 °C lower than the ambient temperature, contributing to a net radiative heat flux away from the collector. This heat transfer process is also influenced by the emissivity of the receiver material and the surface temperature of the absorber. The radiative heat exchange is quantified using the Stefan–Boltzmann law, expressed in Equation (8):

$$\dot{q}\prime_{37rad} = \sigma D_e \pi \varepsilon \left(T_{cub}^4 - T_{ec}^4\right) \tag{8}$$

where σ is the Stefan–Boltzmann constant, De is the external diameter of the receiver, ε is the emissivity of the surface, T_{cub} is the receiver surface temperature, and T_{ec} is the effective sky temperature.

2.3.3. Solar Irradiance Absorbed by the Receiver

To estimate the amount of solar radiation absorbed by the receiver, the model incorporates optical properties, the direct normal irradiance (DNI), and the solar incidence angle. First, the solar irradiance per unit length is calculated using Equation (9). Then, the optical efficiency of the system, using Equation (10). The total absorbed solar irradiance by the receiver is then determined using Equation (11):

$$q_{si} = \frac{DNI \times A_a}{L} \tag{9}$$

$$n_{env} = K(\theta)\varepsilon_1\varepsilon_2\varepsilon_3\varepsilon_4\rho \tag{10}$$

$$\dot{q}'_{3SolAbs} = q_{si} \times n_{env} \times \alpha_{bs} \tag{11}$$

where A_a represents the aperture area of the collector and L is the collector length. The term ε_i denotes a set of optical correction factors that account for various system losses such us including shading, tracking errors, geometric alignment, surface reflectivity, dust accumulation, and other imperfections [32,33] (Table S2), while ρ is the reflectivity of the concentrator and $K(\theta)$ is the incident angle modifier. The product of these terms in Equation (10) yields the effective optical efficiency at the receiver surface, denoted as n_{env}, and α_{bs} is the absorptivity of the receiver surface.

2.3.4. Conduction Losses to Structural Supports

In addition to convective and radiative losses, the model includes conduction losses through the brackets and supports that hold the receiver in place. These losses occur due to temperature gradients between the absorber surface and the collector structure. The heat transfer by conduction to the brackets is calculated using Equation (12) [34]:

$$\dot{q}'_{cond,bracket} = \frac{\sqrt{h_3 P_s k_b A_{ms}}(T_{base} - T_{amb})}{L} \tag{12}$$

where h_3 is the convective heat transfer coefficient for the bracket surface, P_s is the perimeter of contact, k_b is the thermal conductivity of the bracket material, A_{ms} is the minimum contact area, and T_{base} is the temperature at the receiver–bracket interface. The value of h_3 is obtained using the same Zhukauskas correlation used for calculating h_2, but evaluated at the mean temperature between the bracket and ambient air, and based on the external diameter of the receiver.

After defining all the equations describing the heat transfer processes occurring in the system, the model solves the one-dimensional energy balance by iteratively solving for the external surface temperature of the receiver until convergence. This computational module enables the theoretical estimation of the receiver's thermal profile, and the maximum temperature reached based on the geometric configuration.

2.3.5. Solar Ray Tracing and Radiation Distribution

Accurately describing the complex interactions between solar rays, collector geometry, and reflective surfaces is essential for evaluating the optical performance of parabolic trough collectors. These interactions determine how solar radiation is distributed across the absorber and ultimately influence the energy captured by the system. Due to the difficulty of analytically modeling such phenomena, especially under varying sun positions and geometries, researchers recommend the use of computational ray-tracing tools to obtain reliable optical performance data. For this study, SolTRACE v3.0 software was implemented to trace solar ray paths in the selected PTCs [35]. The optical simulation requires a set of input parameters that define the interaction between solar radiation and the

collector's components. These include surface reflectivity, receiver absorptivity, emissivity, transmissivity, and the intercept factor, which accounts for optical precision and alignment quality. The values used in this study are summarized in Table S3.

In Sol TRACE, reflectivity represents the surface's ability to reflect incident solar rays, absorptivity measures how much of the incoming radiation is absorbed by the receiver, and emissivity quantifies how much radiant energy the surface emits relative to a blackbody at the same temperature. These parameters, together, define how efficiently the collector concentrates and converts solar energy.

Another key component of the optical model is the solar incidence angle, which significantly influences the amount of radiation that reaches the receiver (Figure 2 and Table S4). Geometrical variables like the incidence angle, its corresponding correction factor, and the collector's tilt angle play a major role in determining daily and seasonal efficiency. The angle of incidence depends on the collector's orientation, whether it is aligned along a North–South or East–West axis, and on the solar position throughout the day [28].

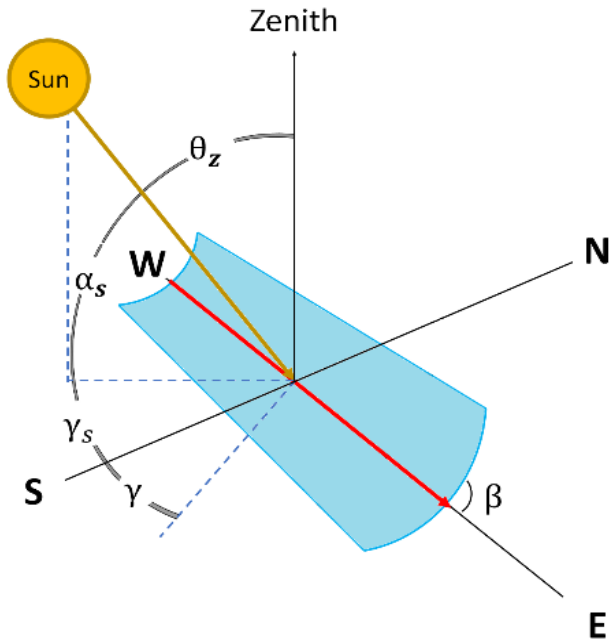

Figure 2. Incident angles on the surface of a parabolic trough collector (PTC). β is the angle between the receiving surface and the horizontal plane; γ_s is the aperture projection angle between the normal of the surface and the local meridian toward the south; θ_z is the incidence angle of direct radiation on a horizontal surface; α_s is the angle between the horizontal and the sun's line.

For a North–South orientation, the incidence angle θ is given by Equation (13):

$$\theta = \cos^{-1}\left(\cos\delta\sqrt{(\cos\phi\cos\omega + \tan\delta\sin\phi)^2 + \sin^2\omega}\right) \tag{13}$$

For an East–West orientation, it is calculated using Equation (14):

$$\theta = \cos^{-1}\left(\sqrt{(1+\cos^2\delta)(\cos^2\omega - 1)}\right) \tag{14}$$

In real operating conditions, solar rays rarely strike the collector at perfect perpendicularity ($\theta \neq 0$). Therefore, it is necessary to account for the optical losses caused by angular deviation, such as the cosine effect and potential shading. These losses are quantified using an incident angle modifier [36], defined by Equation (15):

$$K(\theta) = \cos\theta - 2.86{\cdot}10^{-5}\theta^2 - 5.25{\cdot}10^{-4}\theta \quad (15)$$

Proper collector tilt is essential for maximizing annual solar capture. The optimal tilt angle depends on the site's geographic latitude and should ideally align with the equatorial line. A fixed collector is typically tilted to match the local latitude or slightly offset by ±10°, depending on seasonal priorities. For maximum year-round performance, systems in the Northern Hemisphere should face South, while those in the Southern Hemisphere should be oriented North. Regions within the solar belt (latitudes between 35° N and 35° S) are particularly well-suited for stationary solar collectors due to their high and consistent solar incidence.

2.4. Microbial Inactivation Modelling

The application of parabolic trough collectors (PTCs) in solar water disinfection (SODIS) aims to reduce the microbial load of contaminated water through the synergistic effects of ultraviolet (UV) radiation and thermal energy generated by infrared radiation. This dual mechanism is highly dependent on reactor design, including radiation distribution, velocity profiles, and the geometric dimensions of the system, all of which influence disinfection performance. Environmental conditions are also critical, as they determine the effectiveness of solar water treatment. Parameters such as incident solar irradiance, initial water temperature, and wind speed affect the thermal losses and heat transfer efficiency in both storage containers and SODIS reactor receivers. Additional influencing factors include required solar exposure time, energy dose, water turbidity, dissolved oxygen levels, and the nature of the microorganisms present.

To simulate microbial inactivation under real conditions, a disinfection model was developed based on the empirical formulation to estimate the microbial inactivation rate constant *Kd* as a function of turbidity (TURB, in NTU) and cloud cover (OKTAS) [37] using Equation (16). The rate is calculated using a multiple linear regression model. Values for βi regression coefficients for various turbidity ranges are presented in Table S5.

$$K_d = \beta_0 - \beta_1(TURB) - \beta_2(OKTAS) \quad (16)$$

In addition to optical disinfection modeling, a thermal inactivation sub-model was incorporated. This model estimates the temperature-dependent microbial inactivation rate K_t, assuming no significant thermal inactivation occurs below 45 °C (K_t = 0). For higher temperatures, the rate is defined as follows:

$$K_t = 1.21^{(T-48.3)} \quad (17)$$

The level of microbial inactivation was modeled using a first-order kinetic expression based on Chick's Law, which assumes that the rate of microorganism destruction is proportional to the number of viable organisms, and can be expressed as a logarithmic reduction over time [38,39]. To combine both effects, radiative and thermal, a third model was used to evaluate the logarithmic reduction in microorganisms [40]. This equation accounts for the monochromatic solar intensity $I_{sun}(\lambda)$ ($Wm^{-2}nm^{-1}$), material thickness *Th*, and extinction coefficient $\beta(\lambda)$ (m^{-1}), which depend on the optical properties of the reactor material. The model assumes first-order kinetics and is expressed as:

$$\ln\left(\frac{C}{C_0}\right) = -K{\cdot}I_{sun}(\lambda){\cdot}10^{(-Th\cdot\beta(\lambda))}{\cdot}t \quad (18)$$

where C/C_0 is the microbial concentration ratio, and t is the exposure time in hours.

2.5. Case of Study and Environmental Parameters Assessment

To establish realistic initial conditions across the different modeling modules, a series of evaluation scenarios were developed based on small-scale PTC prototypes and typical environmental conditions in rural and off-grid regions of the Colombian Caribbean. These scenarios aim to validate the feasibility of applying solar thermal collectors for solar water disinfection (SODIS), by simulating pathogen inactivation rates, attainable water temperatures, and thermal performance relative to collector geometry and solar availability. The selected case study focuses on Gambote, Bolívar, a rural settlement located along the banks of the Canal del Dique, where local communities rely on water drawn directly from the canal and nearby lagoons to meet their basic needs. As a derivation of the Magdalena River, the country's main watershed, towards the Caribbean Sea, the Canal del Dique carries high loads of sediments and pollutants, making water quality generally low and exposing the Gambote community to significant environmental health risks [41,42]. The population is composed primarily of ethnic minorities, including Zenú indigenous and Afro-Colombian groups, who rely on traditional, non-dosed water treatment methods. Given the limited access to treated water and reliable sanitation, this community was chosen as a representative site for evaluating the implementation potential of SODIS systems based on glass-free parabolic trough collectors.

Environmental data for this region were obtained from national databases and government meteorological sources, and the modeling process incorporated key variables such as sunshine duration, average ambient temperature, wind speed, peak radiation hours, solar incidence angle, and local water turbidity levels. These parameters were integrated into the simulation workflow to establish realistic boundary conditions for solar exposure, thermal behavior, and microbial inactivation dynamics. Specific values and data sources are provided in the Supplementary Material.

The model was applied under the environmental conditions observed in the study area to evaluate the performance of the selected PTC prototypes, and a sensitivity analysis was carried out considering the variability ranges of key environmental parameters. The objective was to determine the suitability of each prototype for solar disinfection in this region, based on an integrated analysis of multiple factors. These included compact geometric configuration, the ability to reach minimum required disinfection temperatures, volume of water treated, thermal efficiency, concentration ratio, and optical properties. Additionally, exposure time was assessed in relation to the solar incidence angle and prevailing local conditions, allowing a comprehensive evaluation of each design's potential for effective and context-appropriate implementation in rural Caribbean settings.

3. Results and Discussion

3.1. Geometric and Optical Simulation of Selected PTC Prototypes

A total of 16 small-scale parabolic trough collector (PTC) prototypes were selected from the literature to evaluate their suitability for solar water disinfection applications under simplified, glass-free configurations (Table 2). These prototypes vary in terms of aperture width, focal length, rim angle, receiver diameter, and length, reflecting different operational and design objectives such as heat production, disinfection, or residential applications. The geometric model of each prototype is presented in the Supplementary Material (Geometric profiles for selected PTCs).

In parabolic trough collectors, key design parameters include the geometric dimensions and the optical properties of the materials used. These characteristics were analyzed using the proposed model, which integrates each prototype's dimensions and configuration across the different modules to estimate geometric setup, thermal behavior, and radiation

distribution. Notably, parameters such as focal length, rim angle, and collector length vary considerably among prototypes, which directly influences collector efficiency.

Table 2. Geometric Parameters of Selected Small-Scale Parabolic Trough Collector (PTC) Prototypes.

Prototype	Aperture Width (m)	Focal Distance (m)	Rim Angle (°)	Length (m)	Receiver Diameter (mm)	Application	Reference
1	0.80	0.285	70	1.70	0.058	Medium-temperature agro-industrial processes	[43]
2	0.80	0.200	90	0.92	0.025	Nanofluid-based cooling	[44]
3	1.10	0.340	80	3.00	-	Heating applications	[13]
4	1.50	0.450	80	2.50	0.025	Medium- and low-temperature heat generation	[45]
5	1.06	0.266	90	2.44	-	Solar thermal energy production	[46]
6	1.19	0.716	45	4.88	0.025	Steam generation	[47]
7	2.14	0.550	88.5	1.80	0.023	Steam generation	[48]
8	1.74	0.436	90	1.00	0.008	Low-temperature applications	[49]
9	0.50	0.112	96	0.95	0.002	Heating applications	[50]
10	1.00	0.250	90	1.90	0.030	Solar thermal energy production	[51]
11	0.50	0.100	110	1.80	0.010	Residential applications	[52]
12	1.46	0.365	90	2.40	0.027	Low-enthalpy thermal processes	[53]
13	0.80	0.200	90	1.25	0.025		
14	1.06	0.270	90	1.00	0.025		
15	1.67	0.350	100	3.00	0.030		
16	0.70	0.175	90	2.00	-		

The concentration ratio, defined by the relationship between aperture area and receiver area, classifies most of these prototypes as medium- to low-temperature systems, theoretically achieving concentration factors between 5 and 25. These values suggest that operational fluid temperatures between 60 °C and 100 °C are achievable under optimal solar conditions.

Among the 16 documented prototypes, five were selected for detailed thermal analysis based on their representative geometric characteristics. For instance, the prototype 1 [43] features a rim angle of 70° (Figure 3a), which simplifies construction and reduces manufacturing costs. Its design is optimized for stationary operation, showing efficient performance under direct normal irradiance conditions ($\theta = 0°$). A rim angle of 90° offers a more balanced geometry for radiation capture and thermal distribution. Theoretically, this configuration can reach nominal temperatures between 80 °C and 90 °C without the need for a glass envelope, provided that sufficient solar radiation is available. The compact PTC 11 [52] uses a rim angle greater than 90° (Figure 3b), which increases the aperture area and therefore improves its modular application potential. Despite the wider rim angle, its overall dimensions remain suitable for small-scale disinfection systems.

Solar energy capture is highly dependent on the aperture area, which in turn is influenced by both the rim angle and focal distance. A rim angle of 90° is often considered ideal for optimizing geometric concentration. However, optical properties, such as absorptivity and reflectivity, also play a critical role in maximizing solar flux and increasing receiver temperatures. As such, collectors with rim angles ranging between 70° and 110° can still demonstrate strong thermal performance. The ideal PTC design depends largely on the interplay between aperture width and focal distance. A broader aperture generally results in greater thermal output. For compact collectors, it is advisable to maintain an aperture width between 0.5 m and 1.0 m, with receiver diameters sized proportionally. Rim angles between 90° and 110° tend to maximize irradiance along the receiver tube [52]. Furthermore, the receiver diameter may be increased for wider apertures; however, this

also increases convective heat losses. Importantly, the absence of a glass cover does not significantly reduce the global thermal performance, as long as the receiver tube material exhibits low iron content and high absorptivity. Tubular diameters between 25 mm and 50 mm are commonly used for such applications.

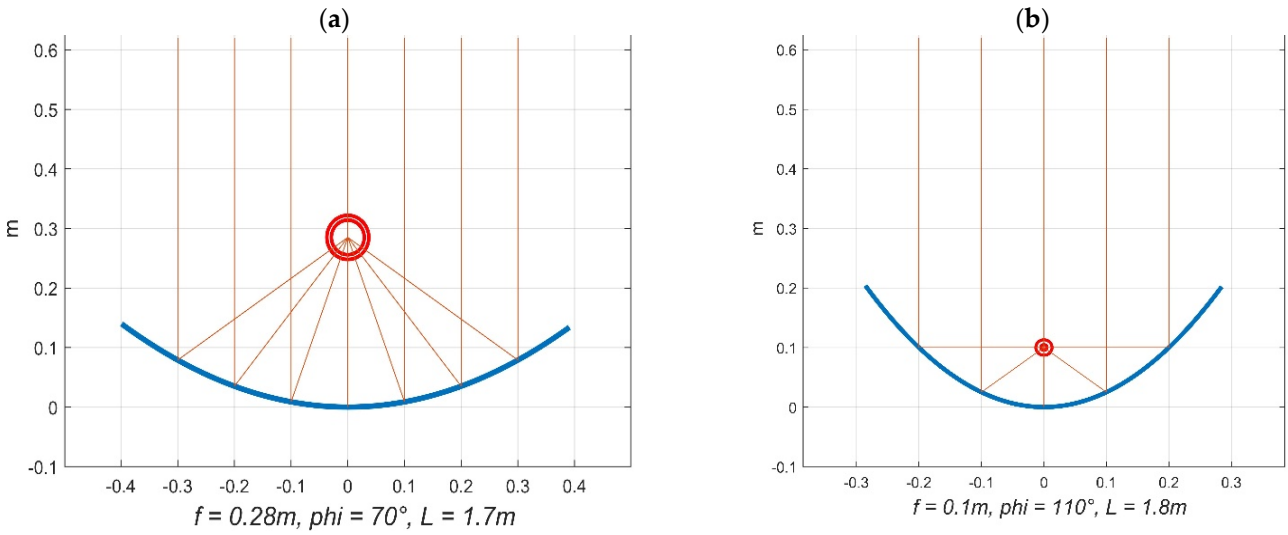

Figure 3. Geometric profile of prototypes 1 (**a**) and 11 (**b**). Concentric circles represent the diameter of the absorber tube located at the focal point of the parabola. The blue line indicates the curved side of the parabolic profile in cross-section. Yellow lines represent incident solar rays striking the parabolic surface perpendicularly and being reflected toward the focal line.

To evaluate how solar energy is distributed across the surface of each prototype, simulations were carried out using SolTrace 3.0, incorporating the key optical properties reflectivity, absorptivity, and emissivity of the materials used. These parameters significantly influence the heat flux distribution, which is governed by the geometric configuration of each collector. Although the main objective is to concentrate solar radiation onto the receiver tube, the simulation results revealed that in several prototypes, a portion of the rays is also focused toward the edges of the reflective surface, leading to radiation losses due to form factor effects and the angle of incidence. As a result, designs with more compact geometries and favorable optical surface performance were prioritized, as they offer better adaptability, reduced material usage, and higher energy concentration on the absorber. These characteristics are critical for maximizing thermal efficiency in glass-free configurations. For example, Figure 4 illustrates how the geometric configuration of prototypes 4 and 12 results in different incident radiation profiles. Prototype 12 shows a higher overall solar input; however, it also exhibits greater thermal concentration at the center. Both configurations reveal energy losses at the edges, highlighting the importance of optimizing the geometry not only for maximum capture but also for uniform distribution. The simulated thermal flux distribution profiles for all 16 prototypes are presented in Supplementary Material (SolTRACE simulation of Heat Distribution on the Surface of the PTC prototypes), providing a general view into how geometry impacts irradiance concentration and edge losses.

3.2. Model Application in the Study Case

The village of Gambote, located in Bolívar, Colombia, offers favorable climatic conditions for implementing solar water disinfection (SODIS) technologies based on glass-free parabolic trough collectors. The region experiences an average ambient temperature of 29 °C, with seasonal highs reaching up to 40 °C, and wind speeds ranging from 1 to 7 m/s.

The site receives approximately 6 h of sunshine per day, and peak solar irradiance typically occurs between 9:00 a.m. and 3:00 p.m., supporting extended daily exposure times. The global solar radiation averages 5.5 kWh/m^2/day, while the monthly solar energy potential can reach 6.5 kWh/m^2, highlighting the area's high insolation. These environmental conditions were used as inputs for the integrated model, which simulated heat transfer dynamics and microbial inactivation processes under realistic operational scenarios [54]. Additionally, local water turbidity, a critical factor influencing optical disinfection efficiency, ranges from 2.54 to 72.9 NTU, requiring flexible system performance across a broad spectrum of water quality levels.

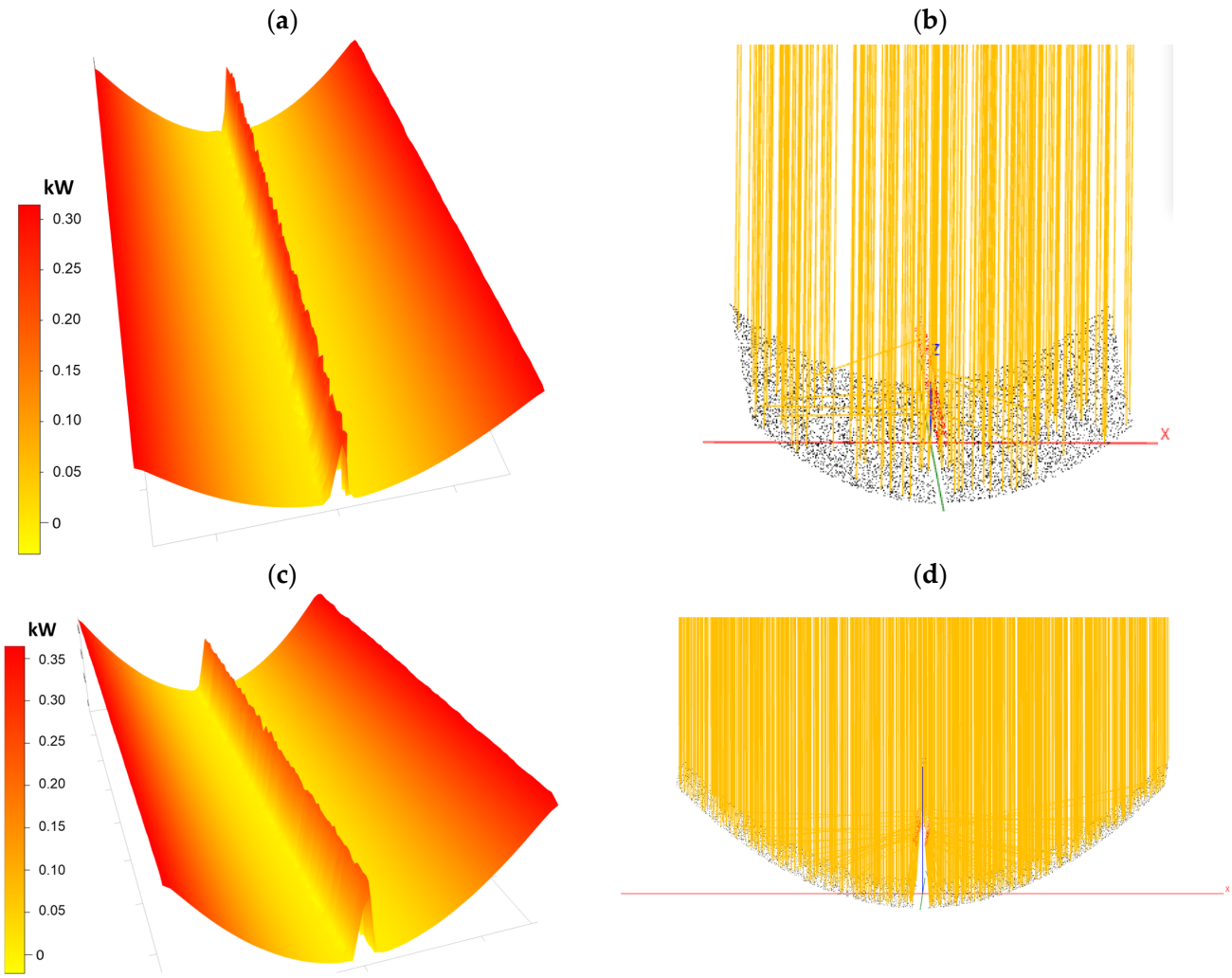

Figure 4. Heat distribution on the surface of prototypes 4 (**a**) and 12 (**c**), and incident solar radiation on the surface of prototypes 4 (**b**) and 12 (**d**), simulated using SolTrace 3.0.

3.2.1. Thermal Performance of Selected PTC Prototypes

Simulation results showed that soft thermal gains, expressed as fluid temperatures, reached values up to 90 °C, depending on the prototype. This range is sufficient for effective microbial reduction, with temperatures of 80 °C inactivating fecal coliforms and 45 °C to 65 °C proving effective for other common pathogens [55] (Table 3). When irradiance exceeds 750 W/m^2 and cloud cover is minimal (0 OKTAS), and assuming a turbidity level of 4.14 NTU, the microbial inactivation rate varies between 2.2 and 3.4 h^{-1} during peak solar hours. In these optimal conditions, a glass-free PTC reactor using a borosilicate receiver tube with 8 mm wall thickness can effectively estimate exposure time required for disinfection.

Table 3. Minimum inactivation temperatures for selected pathogenic microorganisms and parasite stages relevant to solar water disinfection [55].

Microorganisms	Time and Temperature for 100% Elimination		
	1 min	6 min	60 min
Enteroviruses			62 °C
Rotaviruses			63 °C
Fecal coliforms	80 °C		
Salmonella spp.		62 °C	58 °C
Shigella spp.		61 °C	54 °C
Vibrio cholerae			45 °C
Entamoeba spp.	57 °C	54 °C	50 °C
Giardia sp. cysts	57 °C	54 °C	50 °C
Hookworm eggs and larvae		62 °C	51 °C
Ascaris spp. eggs	68 °C	62 °C	57 °C
Schistosoma spp. eggs	60 °C	55 °C	50 °C
Taenia spp. eggs	65 °C	57 °C	51 °C

The exposure time and inactivation rate depend heavily on the solar energy available. During peak hours, higher irradiance leads to shorter required exposure times due to elevated receiver temperatures and increased thermal efficiency. The longitudinal thermal profile of each prototype was assessed using the heat transfer module, enabling a detailed view of temperature distribution along the receiver tube. At 12:00 p.m., the highest solar radiation in the area is observed, during which the prototypes generate temperatures ranging from 40 °C to 135 °C. The hourly radiation profile, temperature distribution by prototype and inactivation rate are presented in Figure S3. Particular attention was given to prototypes capable of reaching temperatures of 70 °C or higher, as this threshold is considered optimal for SODIS efficacy without inducing boiling conditions. Although water boiling can ensure full sterilization, it is not recommended in glass-free systems due to potential pressure buildup within the receiver and safety concerns related to system integrity. Figure 5 shows thermal profiles and concentration factors for selected prototypes.

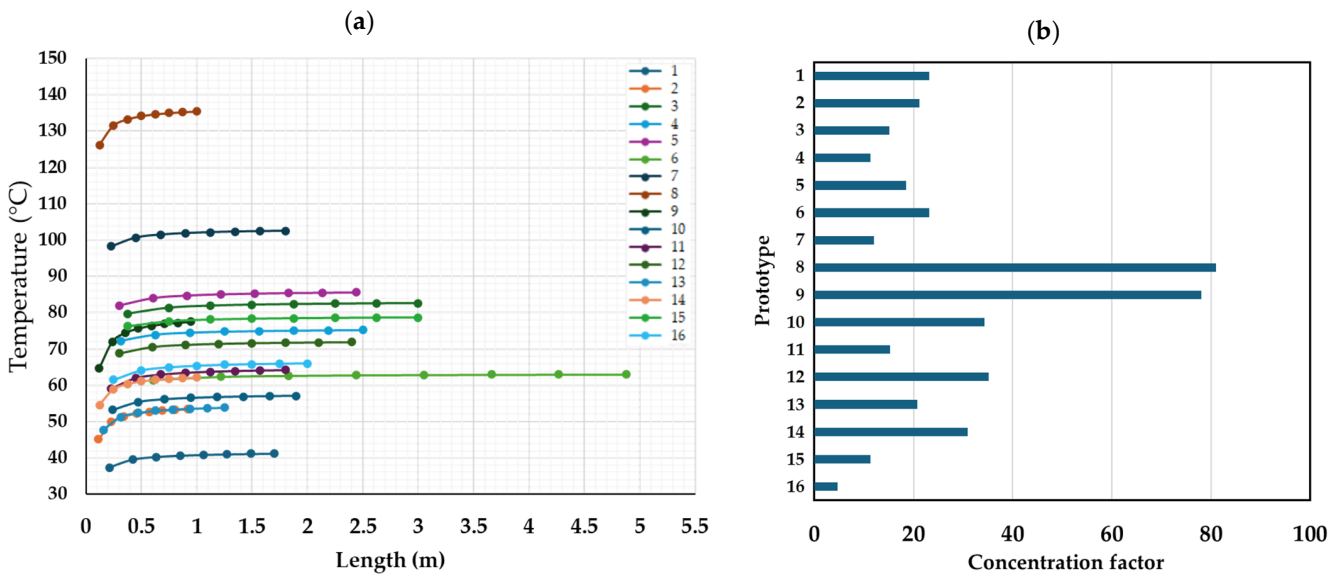

Figure 5. (**a**) Thermal profiles and (**b**) concentration factors for selected PTC prototypes.

Collectors with longer receiver lengths achieve higher temperatures due to increased solar energy absorption. In stagnation-flow collectors, this characteristic allows for greater

heat retention along the entire absorber tube, making it possible to treat larger volumes of water effectively. For continuous-flow systems, this effect supports recirculation processes, enabling the target water volume to reach the necessary temperature and exposure time for disinfection.

Most evaluated prototypes reached the minimum temperature threshold required for effective solar disinfection. Notably, prototypes 7 and 8, despite their compact geometry, demonstrated superior thermal performance. Their design allows for higher operating temperatures, making them well-suited for the selected application scenario. These configurations even offer the potential for steam generation, expanding their utility beyond disinfection. Furthermore, in some cases, a receiver length of just one meter is sufficient to achieve temperatures exceeding 50 °C, which aligns with the thermal resistance limits of most pathogens and initiates thermal inactivation.

A key advantage of parabolic trough collectors lies in their versatility, modularity, and thermal efficiency. According to several studies, PTCs can achieve thermal efficiencies between 70% and 80% (Figure 6). However, in the absence of evacuated tube receivers, these values may decline due to increased convective and radiative losses. The one-dimensional heat transfer model applied here, although limited to collector lengths under 100 m and assuming uniform irradiance along the receiver, provided reliable predictions aligned with expected thermal efficiencies. Still, system performance also depends on additional variables such as collector length, aperture area, and environmental conditions that influence heat losses and useful energy output along the receiver.

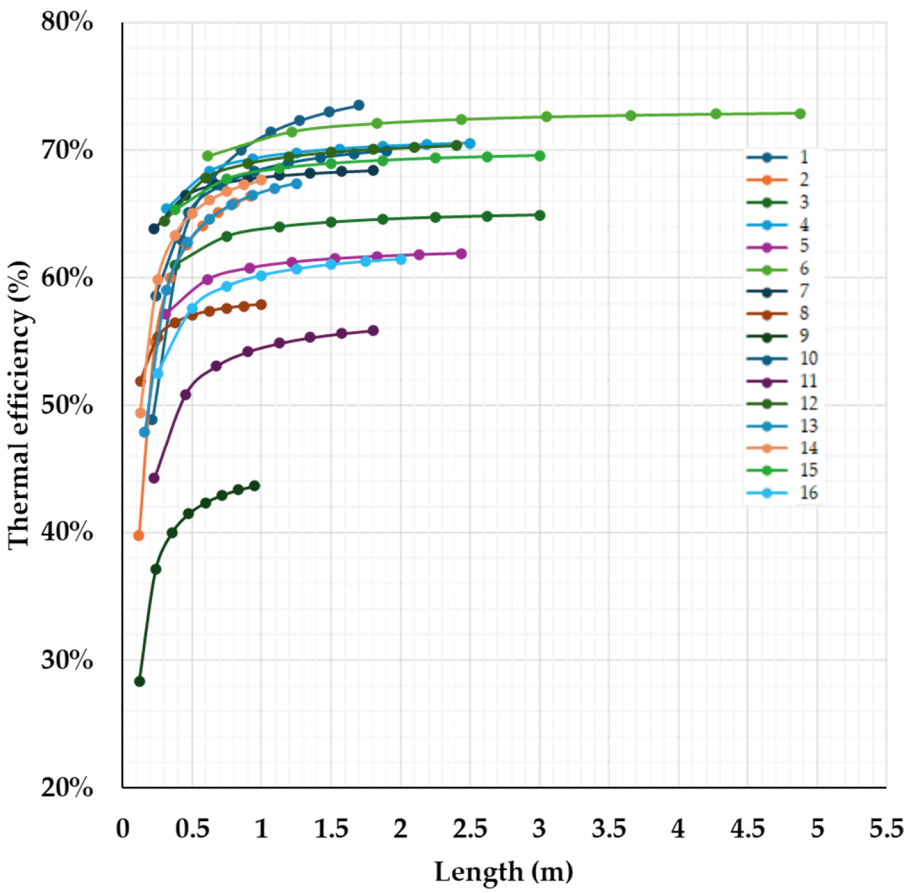

Figure 6. Estimated thermal efficiency of parabolic trough collectors (PTCs) under typical operating condition.

3.2.2. Estimation of Inactivation Rate and Exposure Time for Solar Water Disinfection

Microorganisms are sensitive to ultraviolet (UV) wavelengths ranging from 280 to 320 nm, with shorter wavelengths producing higher inactivation rates. This confirms that solar radiation is effective for pathogen inactivation, particularly when combined synergistically with elevated temperatures. Although photoinactivation processes alone may require long exposure times and are highly dependent on geographic and environmental conditions, the inactivation module developed in this study enables the estimation of kinetic constants that predict microbial reduction and required exposure time under the operational characteristics of a parabolic trough collector. The geometry, optical properties, and thermal capacity of the receiver all contribute to improving disinfection performance. A contaminated water volume containing microorganisms is fed into the receiver tube of the collector, which absorbs solar radiation during peak irradiance hours. The collector functions as a thermal exchanger, generating a longitudinal temperature profile along the receiver and triggering microbial inactivation through a combination of thermal elevation and radiation absorption. The model accounts for ambient environmental conditions and water quality parameters, such as turbidity and initial microbial load.

Simulation results indicate that the evaluated prototypes reach the required temperatures for thermal inactivation, as reflected in their corresponding kinetic rate constants. In conventional SODIS methods, a minimum exposure time of 6 h is typically recommended; this value was used as the initial condition for the proposed model. However, most of the tested devices required as little as 3 h of exposure under low solar potential conditions, such as those typically occurring around 7:00 a.m. During peak solar hours, microbial inactivation was achieved in as little as 30 min, with several prototypes maintaining effective disinfection even at irradiance levels as low as 500 W/m^2.

This analysis also considered the solar incidence angle during predefined evaluation hours in the inactivation module, as well as the thermal profile and geometric configuration of each prototype. Optical properties and receiver thickness (8 mm) were treated as fixed parameters, assuming a borosilicate glass tube [56]. This material enables superior absorption of irradiance and UV-A/UV-B radiation, compared to conventional transparent plastics used in traditional SODIS systems, such as polycarbonate (PC), polypropylene copolymer (PPCO), polystyrene (PS), and polyethylene terephthalate (PET).

Since the kinetic inactivation constants are directly linked to environmental conditions, both thermal and photoinactivation vary over time according to turbidity and the temperature achieved by the collector, which itself depends on solar radiation. In this case, solar irradiance has a greater influence than temperature on microbial inactivation. However, when evaluating disinfection kinetics throughout different hours of the day, the total inactivation rate remained relatively stable, ranging between 1.3 and 2.5 h^{-1}. Prototypes with higher thermal efficiency consistently demonstrated higher inactivation rates, significantly reducing the required exposure time (Figure S3). Under these conditions, the device dimensions primarily determine the volume of water that can be treated.

In rural communities, daily domestic water use is estimated at approximately 100 L per person, with 2.7 to 3.7 L typically allocated for drinking purposes. Among the evaluated prototypes, the volume of water that can be treated using solar disinfection varies based on the receiver's size. While increasing the receiver volume may allow greater treatment capacity, it can also reduce thermal performance. Alternatively, deploying multiple collectors simultaneously can ensure sufficient treated water is available to meet daily consumption needs. An estimation of the treated volume for each prototype is illustrated in Figure 7.

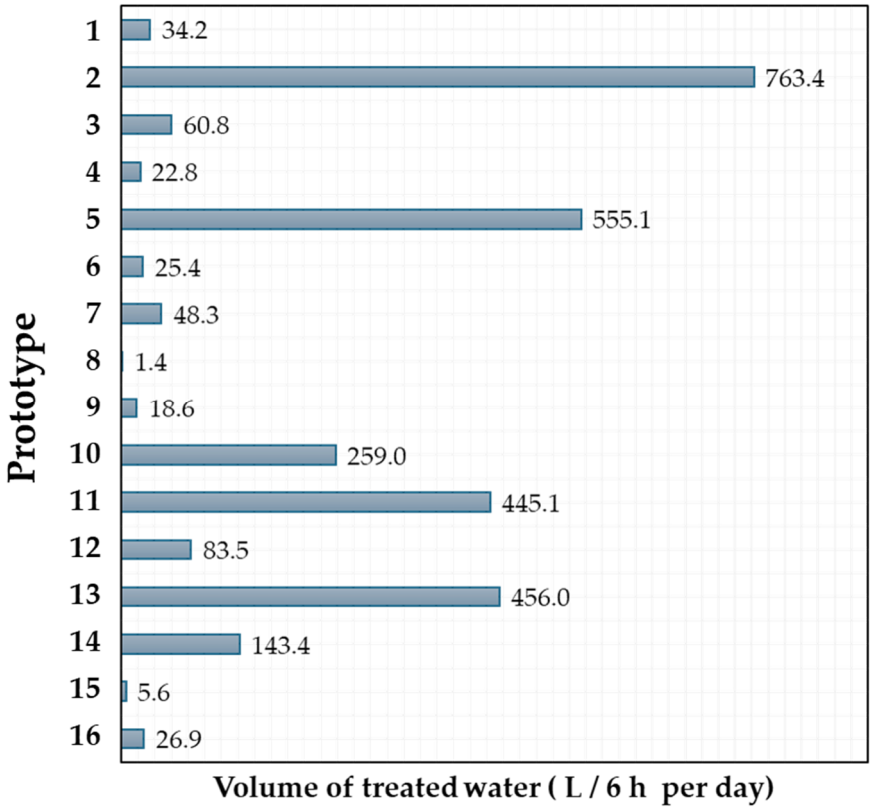

Figure 7. Estimated treated water volume per prototype under rural consumption scenarios.

3.2.3. Sensitivity Analysis of Parabolic Trough Collector Properties

Using the dimensions and geometric configuration of the prototype 7 [48] a sensitivity analysis was performed to evaluate the collector's behavior under design modifications. This analysis focused on the influence of key geometric and environmental variables on thermal performance, solar capture efficiency, and system responsiveness to ambient conditions. A summary of the correlations between significant variables and collector performance outcomes is shown in Figure S4. Among the geometric parameters analyzed, focal distance exhibited a strong influence on performance metrics. As focal length increases, heat transfer losses also increase, despite theoretical gains in surface area and temperature. However, a longer focal length tends to reduce the concentration ratio, which may lead to less uniform heat distribution along the receiver.

The effect of the rim angle was evaluated across a range of 60° to 120°, revealing a directly proportional relationship with key performance variables such as temperature gain, thermal losses, and overall efficiency. Similar results were observed when modifying the receiver length, although in this case the impact was primarily inverse on heat transfer losses. As the component responsible for converting radiation into thermal energy, the receiver diameter also played a critical role. An increase in diameter led to a reduction in the concentration ratio relative to the aperture area and resulted in higher heat losses, ultimately influencing the maximum temperature achieved in the heat transfer fluid.

Environmental conditions, particularly the angle of solar incidence, ambient temperature, and wind speed, were also identified as major factors affecting collector performance. A significant increase in the incidence angle tends to reduce both optical efficiency and thermal output. Likewise, higher wind speeds decrease thermal performance due to intensified convective heat losses at the receiver surface. On the other hand, greater solar energy potential clearly correlates with higher fluid temperatures, as reflected in the model outputs. Consistent with different reports [31,45], the rim angle emerged as the most critical

design parameter. Values above 90° or below 50° affect the focal distance and reduce the concentration ratio, or cause solar rays to scatter inefficiently. Optimal rim angle and focal length values for medium-temperature collectors were identified around 90–110° and 0.47 m, respectively, with an overall collector length between 1–2 m and a recommended receiver diameter of approximately 70 mm.

4. Limitations and Practical Implications

This study is limited by the vast number of existing PTC designs; however, a representative subset of compact, glass-free prototypes was selected for simulation. While the modeling approach was applied to the specific case of Gambote, Bolívar, this site is broadly representative of rural, off-grid communities across the Colombian Caribbean. Future research should focus on field validation of the most promising collector designs identified in this modeling phase, using experimental trials under real environmental conditions. In addition, environmental variability and climate change scenarios could be included in uncertainty analysis to improve model robustness. Practically, the findings support the development of localized protocols for the implementation, use, and transfer of SODIS technologies. This includes addressing challenges related to construction, user awareness, maintenance, and the need for supportive public policies and funding to enable widespread adoption in vulnerable communities.

5. Conclusions

This study demonstrates the potential of glass-free parabolic trough collectors (PTCs) for solar water disinfection in rural, off-grid communities. By integrating geometric, thermal, and microbial inactivation models, we identified key design and environmental factors that influence system performance. Results show that compact PTC prototypes can achieve effective pathogen inactivation under real conditions in the Colombian Caribbean (Gambote, Bolívar). These insights support the adaptation of SODIS technologies to local needs and highlight the importance of accessible, low-cost solutions for safe water access. Furthermore, the proposed model offers a valuable tool for assessing the feasibility and optimization of future PTC implementations in diverse climatic scenarios and community contexts.

Supplementary Materials: The following supporting information can be downloaded at: https://www.mdpi.com/article/10.3390/physchem6010009/s1, Geometric Factors and Design Equations of the Parabolic Trough Collector; Figure S1. Geometric parameters defining a parabolic trough collector; Table S1. Coefficients Based on Reynolds Number Ranges; Table S2. Recommended Optical Correction Factors for Parabolic Trough Collectors; Table S3. Optical Properties of a PTC Used in SolTRACE Simulations; Table S4. Directional Angles of Direct Solar Radiation; Table S5. Constants and Regression Coefficients for Microbial Inactivation as a Function of Water Turbidity; Figure S2. Climatic and meteorological conditions in Gambote, Bolívar, Colombia; Figure S3. Hourly radiation profile (a), temperature distribution by prototype (b) and inactivation rate (c); Figure S4. Summary of Sensitivity Analysis and Correlation of Key Operating Variables in the Parabolic Trough Collector; Figures S5–S20. Geometric profiles for selected PTCs. SolTRACE simulation of Heat Distribution on the Surface of the PTC prototypes. MATLAB Code for assessing PTC design parameters.

Author Contributions: Conceptualization, F.A. and J.P.; methodology, F.A., J.L.G. and J.P.; software, F.A.; validation, A.S.-C., C.D.-M. and J.P.; formal analysis, F.A., A.S.-C., J.L.G. and J.P.; writing—original draft preparation, F.A. and A.S.-C.; writing—review and editing, J.L.G., C.D.-M. and J.P.; funding acquisition, F.A., C.D.-M. and J.P. All authors have read and agreed to the published version of the manuscript.

Funding: This research was funded by the Science and Technology Ministry of Colombia, Grant No. 812 (2018).

Data Availability Statement: Dataset available on reasonable request.

Acknowledgments: The authors thank the Fundación Universitaria Tecnológico Comfenalco—Cartagena (Colombia), the members of the GISAH Research Group (Universidad Tecnológica de Bolívar), and the GIA Research Group for their support during the development of this work.

Conflicts of Interest: The authors declare no conflicts of interest.

References

1. Zhang, Y.; Sivakumar, M.; Yang, S.; Enever, K.; Ramezanianpour, M. Application of Solar Energy in Water Treatment Processes: A Review. *Desalination* **2018**, *428*, 116–145. [CrossRef]
2. Pichel, N.; Vivar, M.; Fuentes, M. The Problem of Drinking Water Access: A Review of Disinfection Technologies with an Emphasis on Solar Treatment Methods. *Chemosphere* **2019**, *218*, 1014–1030. [CrossRef] [PubMed]
3. *WHO Burden of Disease Attributable to Water, Sanitation and Hygiene: 2019 Update*; World Health Organization: Geneva, Switzerland, 2023; Available online: https://www.who.int/publications/i/item/9789240075610 (accessed on 16 April 2025).
4. Ballesteros, M.; Brindley, C.; Sánchez-Pérez, J.A.; Fernández-Ibañez, P. Worldwide Research Trends on Solar-Driven Water Disinfection. *Int. J. Environ. Res. Public Health* **2021**, *18*, 9396. [CrossRef]
5. García-Gil, Á.; García-Muñoz, R.A.; McGuigan, K.G.; Marugán, J. Solar Water Disinfection to Produce Safe Drinking Water. A Review of Parameters, Enhancements, and Modelling Approaches to Make SODIS Faster and Safer. *Molecules* **2021**, *26*, 3431. [CrossRef] [PubMed]
6. Manikandan, G.K.; Iniyan, S.; Goic, R. Enhancing the Optical and Thermal Efficiency of a Parabolic Trough Collector—A Review. *Appl. Energy* **2019**, *235*, 1524–1540. [CrossRef]
7. Hamdan, M.; Al Louzi, R.; Al Aboushi, A.; Abdelhafez, E. Enhancement of Solar Water Disinfection Using Nanocatalysts. *J. Ecol. Eng.* **2022**, *23*, 14–20. [CrossRef]
8. Booshehri, A.Y.; Polo-Lopez, M.I.; Castro-Alférez, M.; He, P.; Xu, R.; Rong, W.; Malato, S.; Fernández-Ibáñez, P. Assessment of Solar Photocatalysis Using Ag/$BiVO_4$ at Pilot Solar Compound Parabolic Collector for Inactivation of Pathogens in Well Water and Secondary Effluents. *Catal. Today* **2017**, *281*, 124–134. [CrossRef]
9. Abdel Dayem, A.M.; El-Ghetany, H.H.; El-Taweel, G.E.; Kamel, M.M. Thermal Performance and Biological Evaluation of Solar Water Disinfection Systems Using Parabolic Trough Collectors. *Desalin. Water Treat.* **2011**, *36*, 119–128. [CrossRef]
10. Cheng, Z.D.; He, Y.L.; Wang, K.; Du, B.C.; Cui, F.Q. A Detailed Parameter Study on the Comprehensive Characteristics and Performance of a Parabolic Trough Solar Collector System. *Appl. Therm. Eng.* **2014**, *63*, 278–289. [CrossRef]
11. Ajbar, W.; Parrales, A.; Silva-Martínez, S.; Bassam, A.; Jaramillo, O.A.; Hernández, J.A. Identification of the Relevant Input Variables for Predicting the Parabolic Trough Solar Collector's Outlet Temperature Using an Artificial Neural Network and a Multiple Linear Regression Model. *J. Renew. Sustain. Energy* **2021**, *13*, 043701. [CrossRef]
12. Kumar, D.; Kumar, S. Thermal Performance of the Solar Parabolic Trough Collector at Different Flow Rates: An Experimental Study. *Int. J. Ambient Energy* **2018**, *39*, 93–102. [CrossRef]
13. Tagle-Salazar, P.D.; Nigam, K.D.P.; Rivera-Solorio, C.I. Heat Transfer Model for Thermal Performance Analysis of Parabolic Trough Solar Collectors Using Nanofluids. *Renew. Energy* **2018**, *125*, 334–343. [CrossRef]
14. Castro-Alférez, M.; Polo-López, M.I.; Marugán, J.; Fernández-Ibáñez, P. Mechanistic Modeling of UV and Mild-Heat Synergistic Effect on Solar Water Disinfection. *Chem. Eng. J.* **2017**, *316*, 111–120. [CrossRef]
15. Manjón, F.; Villén, L.; García-Fresnadillo, D.; Orellana, G. On the Factors Influencing the Performance of Solar Reactors for Water Disinfection with Photosensitized Singlet Oxygen. *Environ. Sci. Technol.* **2008**, *42*, 301–307. [CrossRef]
16. Bellos, E.; Tzivanidis, C. Alternative Designs of Parabolic Trough Solar Collectors. *Prog. Energy Combust. Sci.* **2019**, *71*, 81–117. [CrossRef]
17. Abed, N.; Afgan, I. An Extensive Review of Various Technologies for Enhancing the Thermal and Optical Performances of Parabolic Trough Collectors. *Int. J. Energy Res.* **2020**, *44*, 5117–5164. [CrossRef]
18. Alamdari, P.; Khatamifar, M.; Lin, W. Heat Loss Analysis Review: Parabolic Trough and Linear Fresnel Collectors. *Renew. Sustain. Energy Rev.* **2024**, *199*, 114497. [CrossRef]
19. Wang, Q.; Yang, H.; Hu, M.; Huang, X.; Li, J.; Pei, G. Preliminary Performance Study of a High-Temperature Parabolic Trough Solar Evacuated Receiver with an Inner Transparent Radiation Shield. *Sol. Energy* **2018**, *173*, 640–650. [CrossRef]
20. Kalogirou, S.A. A Detailed Thermal Model of a Parabolic Trough Collector Receiver. *Energy* **2012**, *48*, 298–306. [CrossRef]
21. Reed, R.H. The Inactivation of Microbes by Sunlight: Solar Disinfection as a Water Treatment Process. *Adv. Appl. Microbiol.* **2004**, *54*, 333–365. [CrossRef]

22. Manfrida, G.; Petela, K.; Rossi, F. Natural Circulation Solar Thermal System for Water Disinfection. *Energy* **2017**, *141*, 1204–1214. [CrossRef]
23. El Kouche, A.; Ortegón Gallego, F. Modeling and Numerical Simulation of a Parabolic Trough Collector Using an HTF with Temperature Dependent Physical Properties. *Math. Comput. Simul.* **2022**, *192*, 430–451. [CrossRef]
24. Marif, Y.; Benmoussa, H.; Bouguettaia, H.; Belhadj, M.M.; Zerrouki, M. Numerical Simulation of Solar Parabolic Trough Collector Performance in the Algeria Saharan Region. *Energy Convers. Manag.* **2014**, *85*, 521–529. [CrossRef]
25. Madadi Avargani, V.; Rahimi, A.; Divband, M. Coupled Optical and Thermal Analyses of a New Type of Solar Water Heaters Using Parabolic Trough Reflectors. *Sustain. Energy Technol. Assess.* **2020**, *40*, 100780. [CrossRef]
26. Barbón, A.; Vesperinas, D.; Bayón, L.; García-Mollaghan, D.; Ghodbane, M. Numerical Simulation of a Solar Water Disinfection System Based on a Small-Scale Linear Fresnel Reflector. *RSC Adv.* **2022**, *13*, 155–171. [CrossRef]
27. Forristall, R. *Heat Transfer Analysis and Modeling of a Parabolic Trough Solar Receiver Implemented in Engineering Equation Solver*; NREL/TP-550-34169; National Renewable Energy Lab: Golden, CO, USA, 2003; p. 164.
28. Duffie, J.A.; Beckman, W.A.; McGowan, J. Solar Engineering of Thermal Processes. *Am. J. Phys.* **1985**, *53*, 382. [CrossRef]
29. Kalogirou, S.A. Solar Thermal Collectors and Applications. *Prog. Energy Combust. Sci.* **2004**, *30*, 231–295. [CrossRef]
30. Keou, C.-J.N.; Njomo, D.; Sambou, V.; Finiavana, A.R.A.; Tidiane, A.D. Two-Dimension Numerical Simulation of Parabolic Trough Solar Collector: Far North Region of Cameroon. *Energy Power Eng.* **2017**, *9*, 147–169. [CrossRef]
31. Cheng, Z.D.; He, Y.L.; Cui, F.Q.; Du, B.C.; Zheng, Z.J.; Xu, Y. Comparative and Sensitive Analysis for Parabolic Trough Solar Collectors with a Detailed Monte Carlo Ray-Tracing Optical Model. *Appl. Energy* **2014**, *115*, 559–572. [CrossRef]
32. Xu, C.; Chen, Z.; Li, M.; Zhang, P.; Ji, X.; Luo, X.; Liu, J. Research on the Compensation of the End Loss Effect for Parabolic Trough Solar Collectors. *Appl. Energy* **2014**, *115*, 128–139. [CrossRef]
33. Islam, M.; Miller, S.; Yarlagadda, P.; Karim, A. Investigation of the Effect of Physical and Optical Factors on the Optical Performance of a Parabolic Trough Collector. *Energies* **2017**, *10*, 1907. [CrossRef]
34. Incropera, F.; DeWitt, D.; Bergman, T.; Lavine, A. *Fundamentals of Heat and Mass Transfer*; Wiley: New York, NY, USA, 1996.
35. Wendelin, T. SolTRACE: A New Optical Modeling Tool for Concentrating Solar Optics. *Int. Sol. Energy Conf.* **2009**, *36762*, 253–260. [CrossRef]
36. Carvalho, M.J.; Horta, P.; Mendes, J.F.; Pereira, M.C.; Carbajal, W.M. Incidence Angle Modifiers: A General Approach for Energy Calculations. In *Proceedings of the ISES Solar World Congress 2007*; ISES: Freiburg, Germany, 2007; Volume 1, pp. 608–612.
37. Haider, H.; Ali, W.; Haydar, S.; Tesfamariam, S.; Sadiq, R. Modeling Exposure Period for Solar Disinfection (SODIS) under Varying Turbidity and Cloud Cover Conditions. *Clean Technol. Environ. Policy* **2014**, *16*, 861–874. [CrossRef]
38. Peleg, M. Modeling the Dynamic Kinetics of Microbial Disinfection with Dissipating Chemical Agents—A Theoretical Investigation. *Appl. Microbiol. Biotechnol.* **2021**, *105*, 539–549. [CrossRef]
39. Lamore, Y.; Beyene, A.; Fekadu, S.; Megersa, M. Solar Disinfection Potentials of Aqua Lens, Photovoltaic and Glass Bottle Subsequent to Plant-Based Coagulant: For Low-Cost Household Water Treatment Systems. *Appl. Water Sci.* **2018**, *8*, 100. [CrossRef]
40. García-Gil, Á.; Abeledo-Lameiro, M.J.; Gómez-Couso, H.; Marugán, J. Kinetic Modeling of the Synergistic Thermal and Spectral Actions on the Inactivation of Cryptosporidium Parvum in Water by Sunlight. *Water Res.* **2020**, *185*, 116226. [CrossRef]
41. Romero-Murillo, P.; Gallego, J.L.; Leignel, V. Marine Pollution and Advances in Biomonitoring in Cartagena Bay in the Colombian Caribbean. *Toxics* **2023**, *11*, 631. [CrossRef]
42. Tirado Munoz, O.; Ballestas, I.T.; Valdelamar Villegas, J.C.; Castro Angulo, I. Annual Behavior of Cu, Pb, Cr and Total Hg in Superficial Waters from Dique Channel during 2006-2010, Cartagena, Colombia. *Hydrol. Curr. Res.* **2017**, *8*, 1000279. [CrossRef]
43. Barbosa, E.G.; Martins, M.A.; Viana de Araujo, M.E.; Renato, N.d.S.; Zolnier, S.; Pereira, E.G.; de Oliveira Resende, M. Experimental Evaluation of a Stationary Parabolic Trough Solar Collector: Influence of the Concentrator and Heat Transfer Fluid. *J. Clean. Prod.* **2020**, *276*, 124174. [CrossRef]
44. Palacios, A.; Amaya, D.; Ramos, O. Modeling and Thermal Analysis of a CCP Collector System Based on Fractal Architecture: Receiver Proposal. In *E3S Web of Conferences*; EDP Sciences: Les Ulis, France, 2019; Volume 122.
45. Bharti, A.; Paul, B. Design of Solar Parabolic Trough Collector. In Proceedings of the 2017 International Conference on Advances in Mechanical, Industrial, Automation and Management Systems (AMIAMS), Allahabad, India, 3–5 February 2017; pp. 302–306. [CrossRef]
46. Mentado Islas, D.; Elizalde Carrizo, S.; Jiménez Islas, D.; Azuara Jiménez, J. Simulación de Un Concentrador Solar de Canal Parabólico Mediante El Software SolTrace. *Rev. Prototipos Tecnológicos* **2016**, *2*, 68–75.
47. Hachicha, A.A. Numerical Simulation of a Parabolic Trough Solar Collector for Hot Water and Steam Generation. *AIP Conf. Proc.* **2016**, *1734*, 070013. [CrossRef]
48. César Vera, T. Diseño de Un Colector Parabólico Solar Para La Generación de Vapor. *Investig. Apl. E Innovación* **2016**, *10*, 28–33.

49. May Tzuc, O.; Vázquez Caamal, M.; Bassam, A.; Escalante Soberanis, M.A.; Flota-Bañuelos, M. Implementación de Algoritmos Para Dimensionamiento y Caracterización de Concentradores Solares de Canal Parabólico En Interfaz Computacional. *Abstr. Appl.* **2016**, *14*, 45–56.
50. Macedo-Valencia, J.; Ramírez-Ávila, J.; Acosta, R.; Jaramillo, O.A.; Aguilar, J.O. Design, Construction and Evaluation of Parabolic Trough Collector as Demonstrative Prototype. *Energy Procedia* **2014**, *57*, 989–998. [CrossRef]
51. Ahmed Yassen, T. Experimental and Theoretical Study of a Parabolic Trough Solar Collector. *Anbar J. Eng. Sci.* **2012**, *5*, 109–125. [CrossRef]
52. Salvestroni, M.; Pierucci, G.; Fagioli, F.; Pourreza, A.; Messeri, M.; Taddei, F.; Hosouli, S.; Rashidi, H.; Lucia, M. De Design of a Small Size PTC: Computational Model for the Receiver Tube and Validation with Heat Loss Test. *IOP Conf. Ser. Mater. Sci. Eng.* **2019**, *556*, 012025. [CrossRef]
53. Coccia, G.; Nicola, G.D.; Hidalgo, A. *Parabolic Trough Collector Prototypes for Low-Temperature Process Heat: Springer Briefs in Applied Sciences and Technology*; Springer International Publishing: Cham, Switzerland, 2016.
54. Hurtado Moreno, G.; González, O.C.; Cadena, M.; Benavides, H.; Rúiz, F.; Montealegre, E.; Ortiz Royero, J.C.; Montoya Ramírez, R.D. *Atlas Climatológico de Colombia*, 2nd ed.; Instituto de Hidrología Meteorología y Estudios Ambientales IDEAM, Ed.; IDEAM: Bogotá, DC, Colombia, 2017.
55. Sommer, B.; Mariño, A.; Solarte, Y.; Salas, M.L.; Dierolf, C.; Valiente, C.; Mora, D.; Rechsteiner, R.; Setter, P.; Wirojanagud, W.; et al. SODIS—An Emerging Water Treatment Process. *J. Water Supply Res. Technol.-AQUA* **1997**, *46*, 127–137.
56. Acra, A.; Karahagopian, Y.; Raffoul, Z.; Dajani, R. Disinfection of Oral Rehydration Solutions by Sunlight. *Lancet* **1980**, *316*, 1257–1258. [CrossRef]

Disclaimer/Publisher's Note: The statements, opinions and data contained in all publications are solely those of the individual author(s) and contributor(s) and not of MDPI and/or the editor(s). MDPI and/or the editor(s) disclaim responsibility for any injury to people or property resulting from any ideas, methods, instructions or products referred to in the content.